Electronic Supplementary Material (ESI) for RSC Advances.

Supporting Information

Highly dispersed Ni nanoparticles on mesoporous silica nanospheres by melt infiltration for transfer hydrogenation of aryl ketones

Hyemin Kweon‡[a], Sanha Jang‡[a], Akerke Bereketova[a], Ji Chan Park*[b], and Kang Hyun Park*[a]

[a]Department of Chemistry, Pusan National University, Busan,609-735, Korea.

[b]Clean Fuel Laboratory, Korea Institute of Energy Research, 152 Gajeong-Ro, Daejeon, 305-343, Korea

Hyemin Kweon[a]
[a]E-mail address: hyeminkweon@gmail.com
Sanha Jang[a]
[a]E-mail address: jangs0522@pusan.ac.kr
Akerke Bereketova[a]
[a]E-mail address: akerke07@gmail.com
Ji Chan Park*[b]
[b]E-mail address: jcpark@kier.re.kr, Tel: +82-42-860-3605
Kang Hyun Park*[a]
*[a]Corresponding author: Tel: +82 51 510 2238, fax: +82 51 980 5200 E-mail address: chemistry@pusan.ac.kr
‡ These authors contributed equally to this work.

Chemicals

Nickel(II) nitrate hexahydrate ($Ni(NO_3)_2·6H_2O$, 99.999%), tetraethyl orthosilicate (TEOS, 98%), and cetrimonium bromide ($C_{16}TAB$, ≥98%), acetophenone (99%), isopropanol (99.9%) were purchased from Aldrich. Nickel-aluminum alloy (Ni_3Al) was purchased from Lancaster. Ammonium hydroxide (NH_4OH, 28% in water) and ethanol (99.9%) were obtained from Junsei and J. T. Baker, respectively. The reagents were used as received without further purification.

Preparation of $mSiO_2$ nanosphere

$C_{16}TAB$ (6.0 g, 16.5 mmol) was dissolved in a solution containing distilled water (300 mL), ammonia (28 wt% in water, 4.0 mL) and ethanol (200 mL), and then stirred for 1 h at room temperature. TEOS (8.0 mL) was added to the prepared solution and stirred at 200 rpm for 10 h under an ambient condition. The silica particles were precipitated by centrifugation at 8,000 rpm for 10 min, and then, washed with ethanol. After drying at room temperature for 20 h, the white powder was placed in an alumina boat in a tube-type furnace, heated at a ramping rate of 4.4 $°C·min^{-1}$ to 550 °C, and calcined at the same temperature for 6 h in air in order to remove the remaining surfactant.

Preparation of Ni@$mSiO_2$ nanocatalyst

For synthesis of the Ni (10 wt%)@$mSiO_2$ nanocatalyst, $Ni(NO_3)_2·6H_2O$ (275 mg, 0.95 mmol) and $mSiO_2$ powder (500 mg, 8.3 mmol) were uniformly ground in a mortar for 5 min. After grinding under an ambient condition, the resulting green powder was aged at 60 °C in a tumbling oven. After aging for 24 h, the cooled sample at room temperature was transferred to an alumina boat in a tube-type furnace. Finally, the nickel-incorporated silica powder was slowly heated at a ramping rate of 4 °C·min^{-1} up to 500 °C under a H_2 flow of 200 mL·min^{-1} and maintained at the same temperature for 4 h under a continuous flow of H_2. After thermal reduction, the resulting black powder was cooled down to room temperature and immediately submerged in ethanol (35 mL) under a flow of N_2 (1.0 L·min^{-1}) in order to minimize surface oxidation of the nickel particles. The Ni (10 wt%)@mSiO_2 powder immersed in ethanol was simply separated by a magnet and dried in a vacuum oven at 60 °C.

Characterization

A high-resolution TEM (HRTEM) analysis was performed using a Tecnai TNiF30 ST and a Titan Double Cs corrected TEM instrument (Titan cubed G2 60-300). Energy-dispersive X-ray spectroscopy (EDS) elemental mapping data were collected using a high-efficiency detection system (Super-X detector). For the TEM analysis, the samples were prepared by putting a few drops of the corresponding colloidal solutions on Formvar carbon-coated copper grid and lacey carbon grid (Ted Pellar, Inc). X-ray photoelectron spectroscopy (XPS) spectra were measured using a K-alpha plus (Thermo) with a monochromated Al-Kα (hv = 1486.6 eV)) as the X-ray source with a pass energy of 50.0eV and a step size of 0.1 eV. High-power X-ray powder diffraction (XRD) (Rigaku D/MAX-2500, 18 kW) was also used for the analysis. Hydrogen chemisorption measurement was carried out using a Micromeritics ASAP 2020 C. Before measurement, the sample was heated in flowing hydrogen gas to 400 °C and was held at the same temperature for 8 h. The H_2 adsorption isotherm was measured at 35 °C. Nitrogen sorption isotherms were measured at −196 °C with a Tristar II

3020 surface area analyzer. Before the measurements, the samples were degassed in vacuum at 300 °C for 4 h.

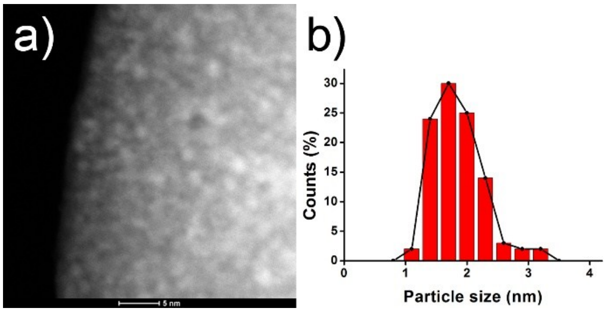

Fig. S1 (a) HAADF image (bars: 5nm) and (b) the size distribution of nickel nanoparticles of Ni@mSiO$_2$.

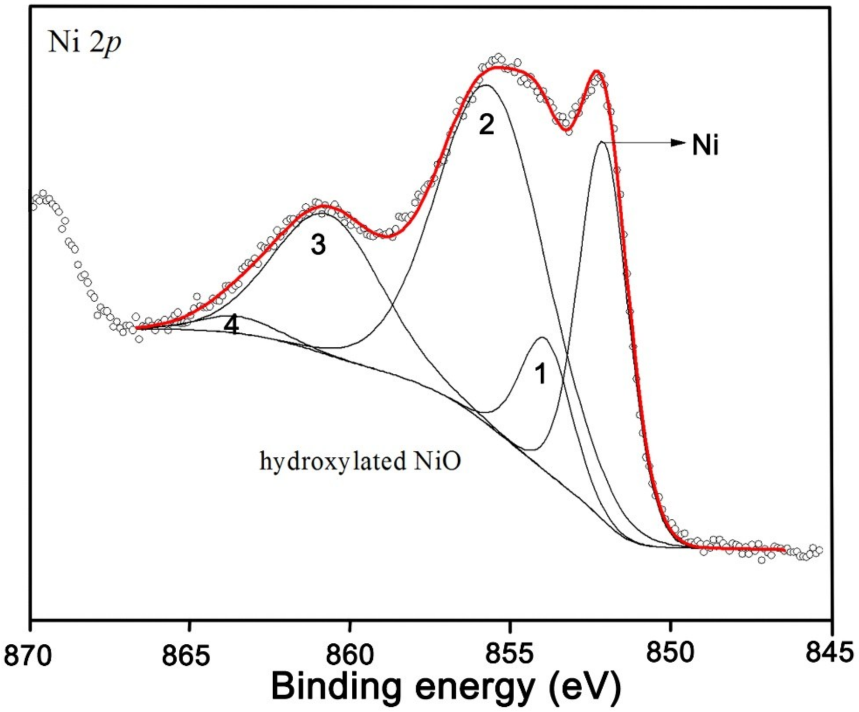

Fig. S2 The XPS spectra of Ni@mSiO$_2$ at Ni peak.

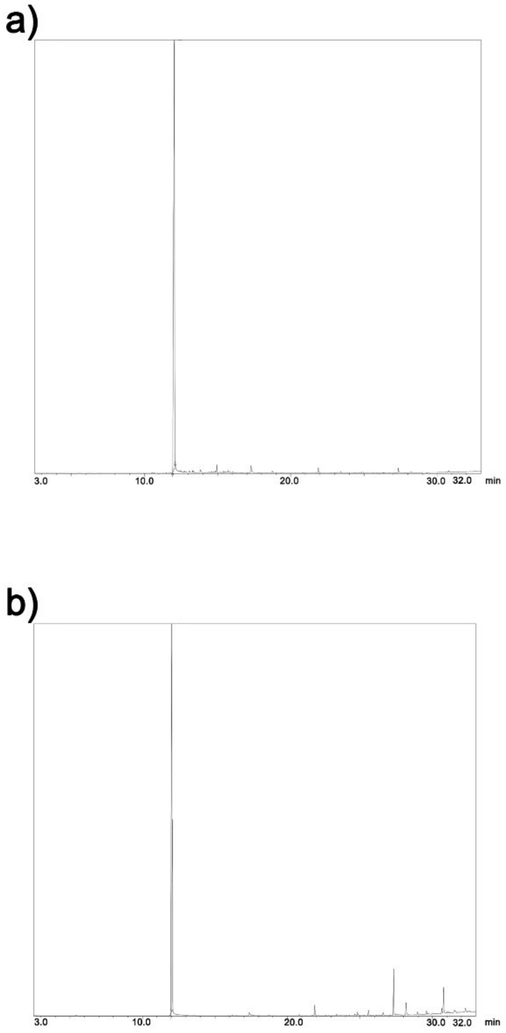

Fig. S3 GC spectra of transfer hydrogenation using (a) Ni@mSiO$_2$, (b) nickel-aluminium alloy catalyst. Acetopheneone and 1-phenylethanol was detected at 12.02min, 12.07 min each.

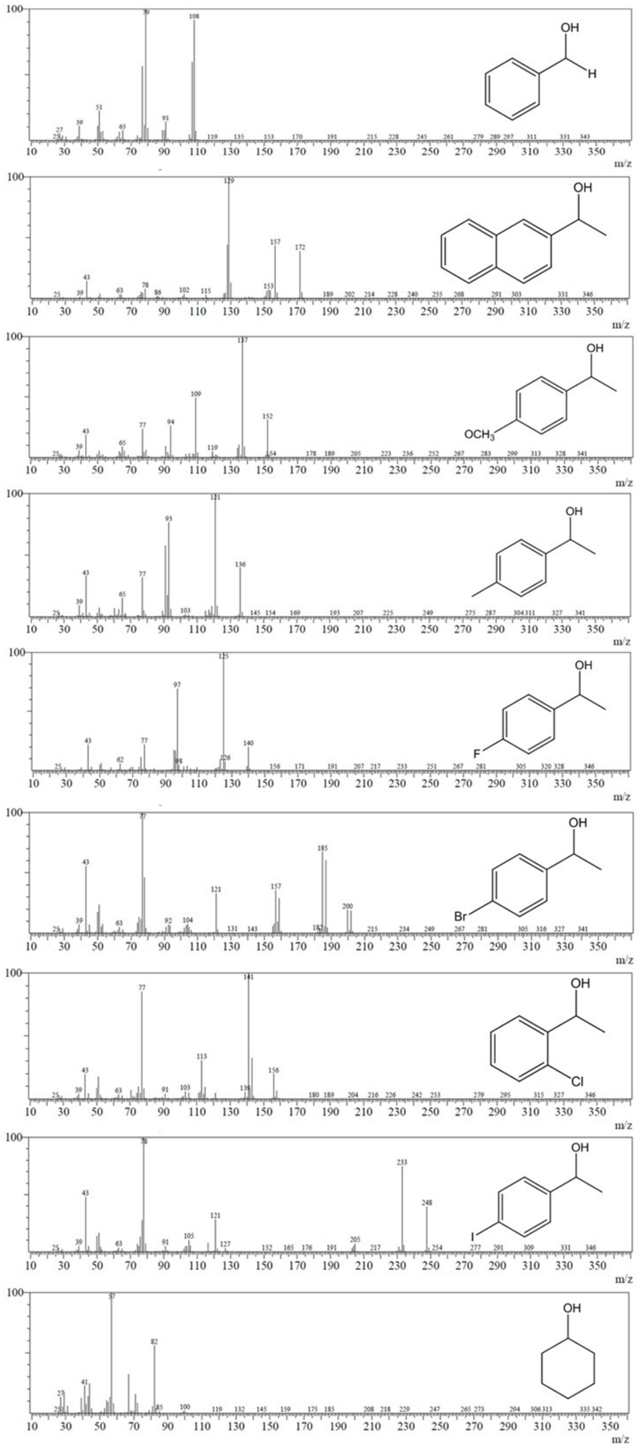

Fig. S4 MS Spectra of various compounds of Table 2.

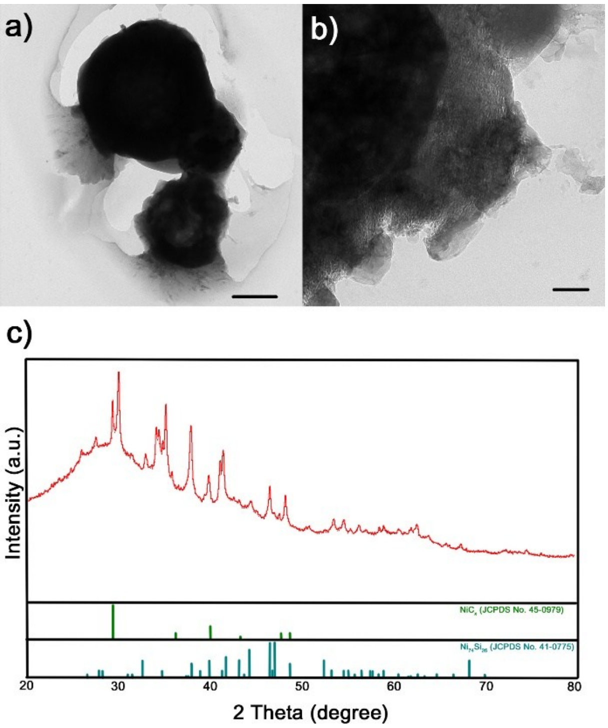

Fig. S5 (a-b) TEM images, (c) XRD spectrum of Ni@mSiO_2 catalyst after reuse. The bars represent 500 nm (a), 100 nm (b).

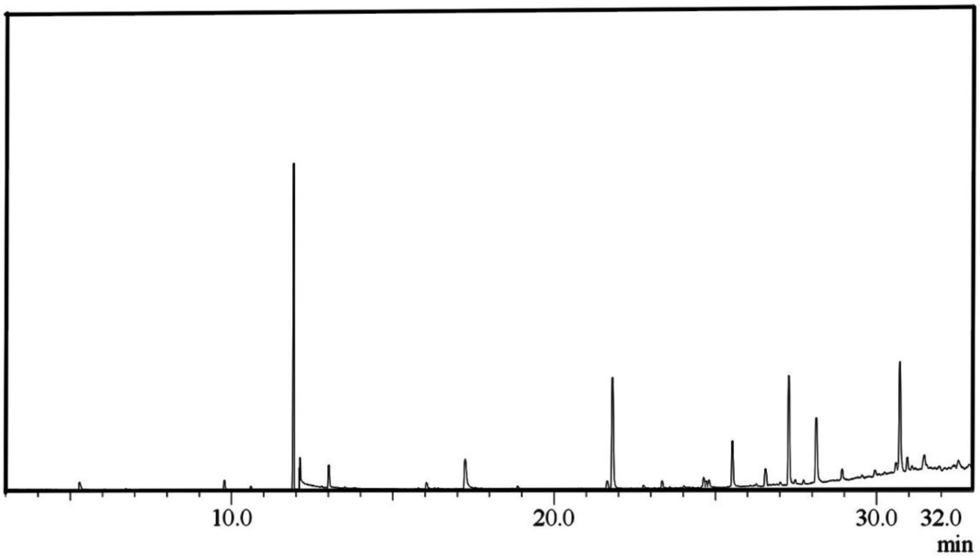

Fig. S6 GC spectra of transfer hydrogenation using recycle of Ni@mSiO_2 catalyst. Acetophenone and 1-phenylethanol was detected at 11.93 min, 12.12 min each.

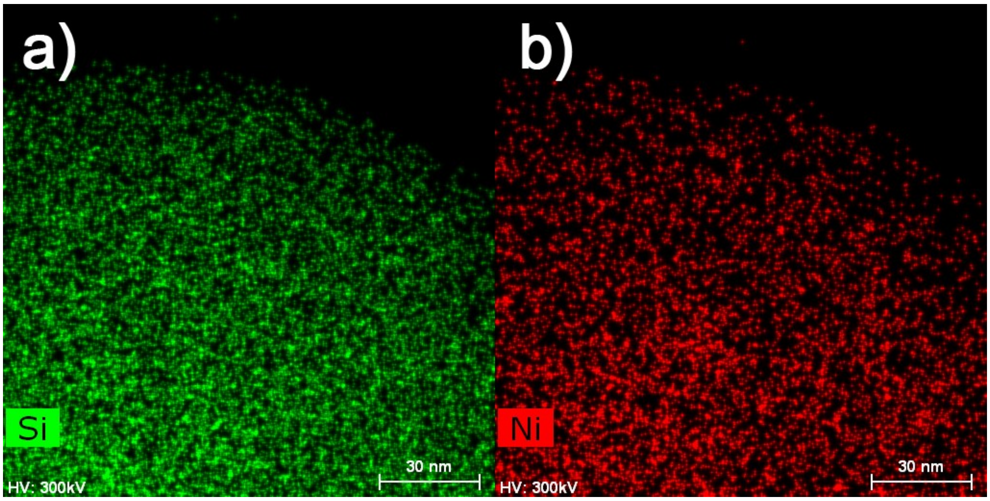

Fig. S7 Scanning TEM images with elemental mapping a) Si and b) Ni.

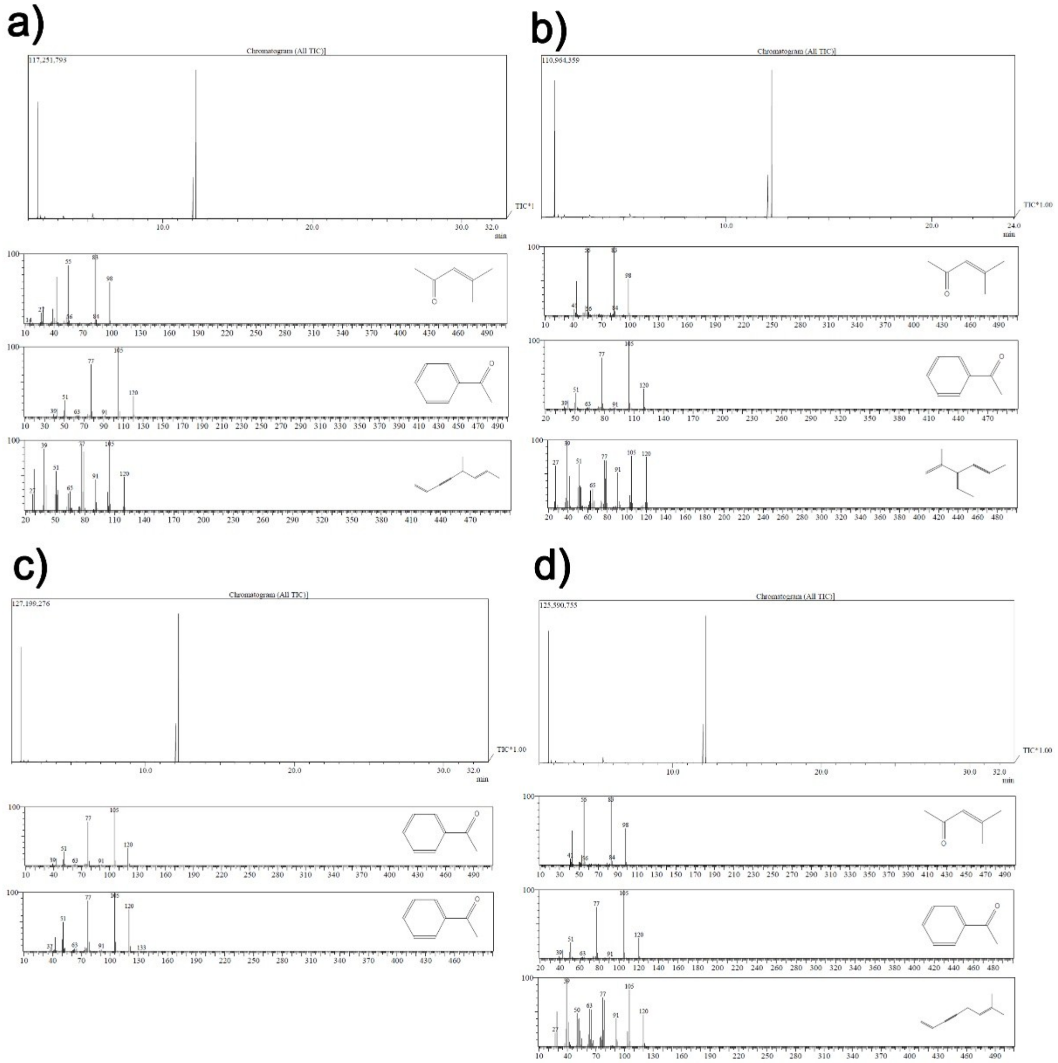

Fig. S8 GC spectra of transfer hydrogenation using a) without Ni@SiO$_2$, b) mSiO$_2$, c) Ni salt@mSiO$_2$, and d) Ni salt, respectively.

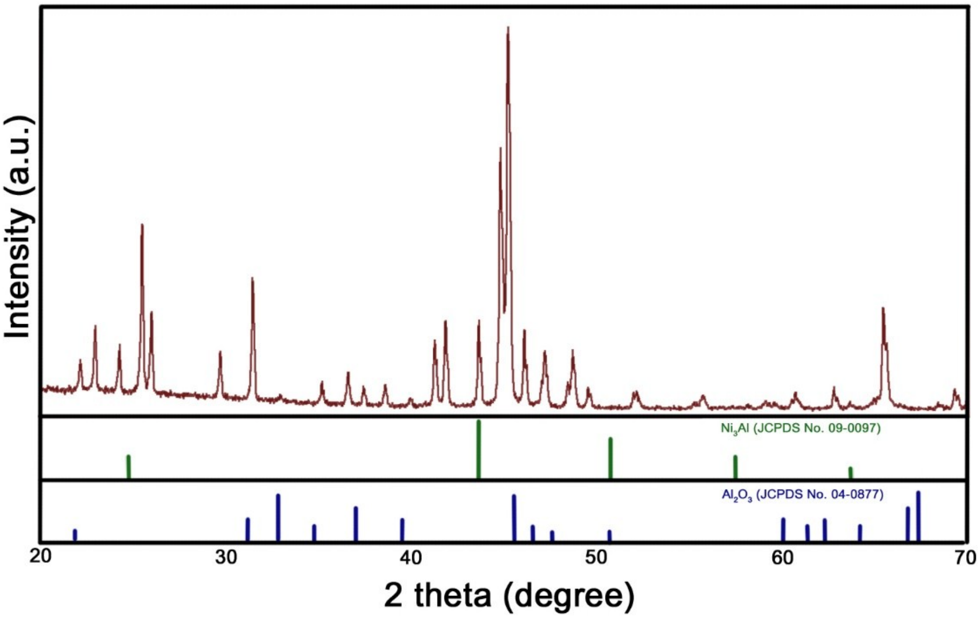

Fig. S9 XRD spectrum of nickel-aluminium alloy

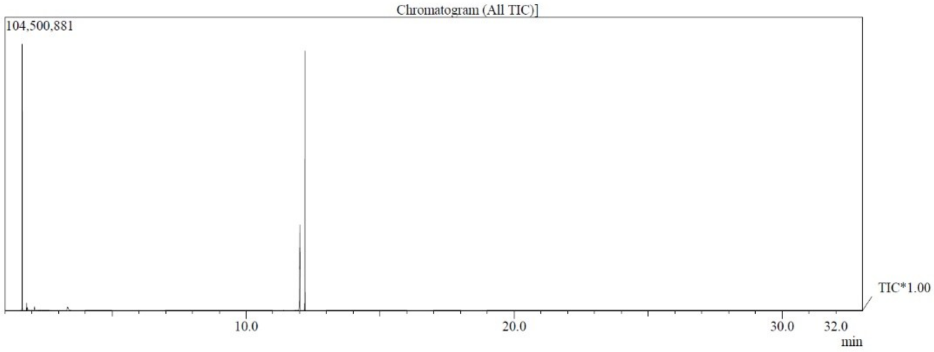

```
                                       Peak Report TIC
  Peak#     R.Time      I.Time      F.Time        Area     Area%       Height   Height%       A/H  Mark
      1     12.013      11.950      12.030    41517528     57.01     30640836     24.84      1.35
      2     12.200      12.180      12.215    31305321     42.99     92704735     75.16      0.34    V
                                              72822849    100.00    123345571    100.00
```

Fig. S10 GC spectra of transfer hydrogenation using recycle of Ni@mSiO_2 catalyst after reduction. Acetophenone and benzaldehyde oxime was detected at 12.013 min, 12.200 min each.

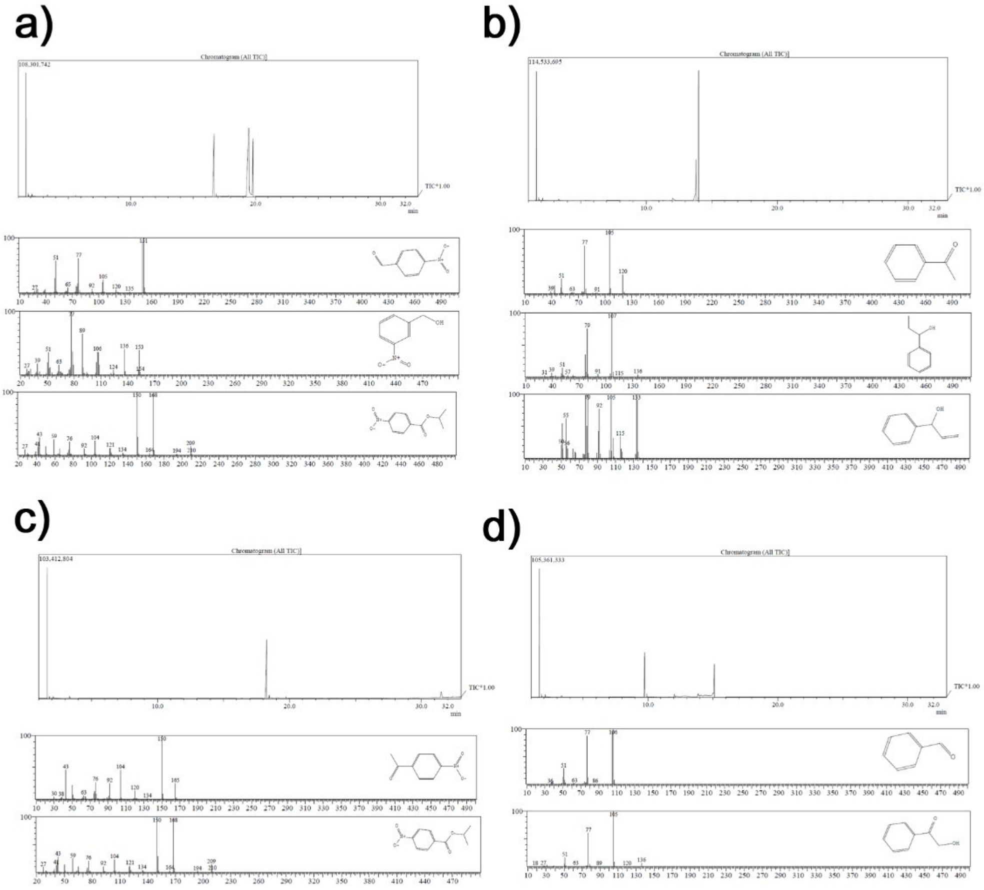

Fig. S11 GC spectra of transfer hydrogenation of various reactant using Ni@mSiO$_2$ nanocatalyst. a) 4-nitrobenzaldehyde, b) propiopheone, c) 4-nitroacetopheone, and d) 2-hydroxyacetopheone.

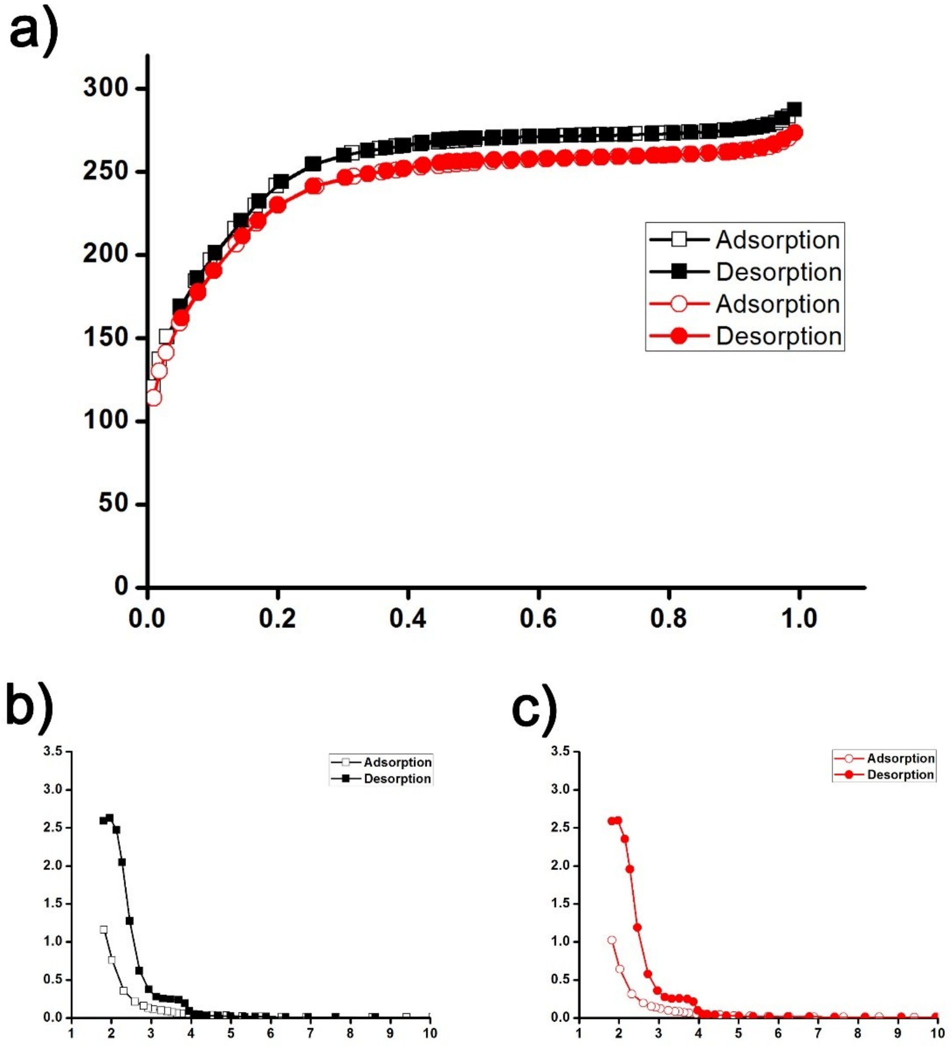

Fig. S12 (a) N_2 adsorption/desorption isotherms of 500 ℃ (black) and 600 ℃ (red) of $mSiO_2$ and (b, c) pore size distribution diagrams of 500 ℃ and 600 ℃ of $mSiO_2$, respectively.

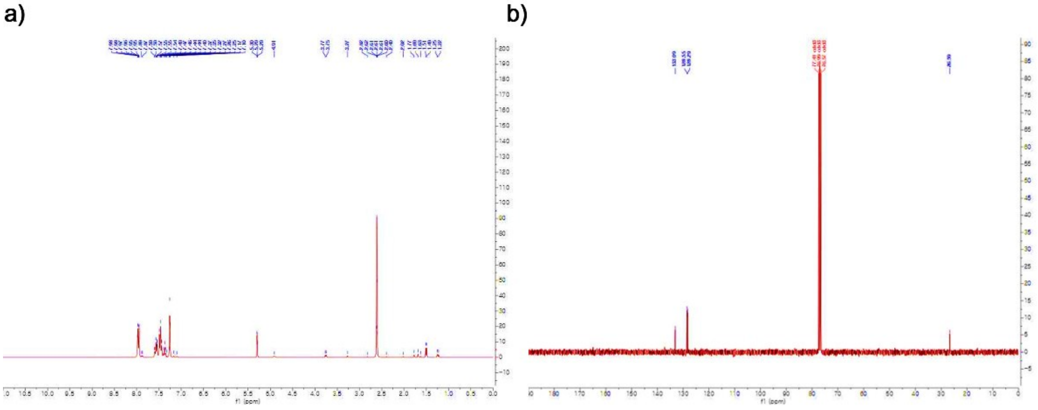

Fig. S13 NMR spectrum of acetophenone and 1-phenylethanol a) ^{1}HNMR and b) ^{13}CMNR, respectively.

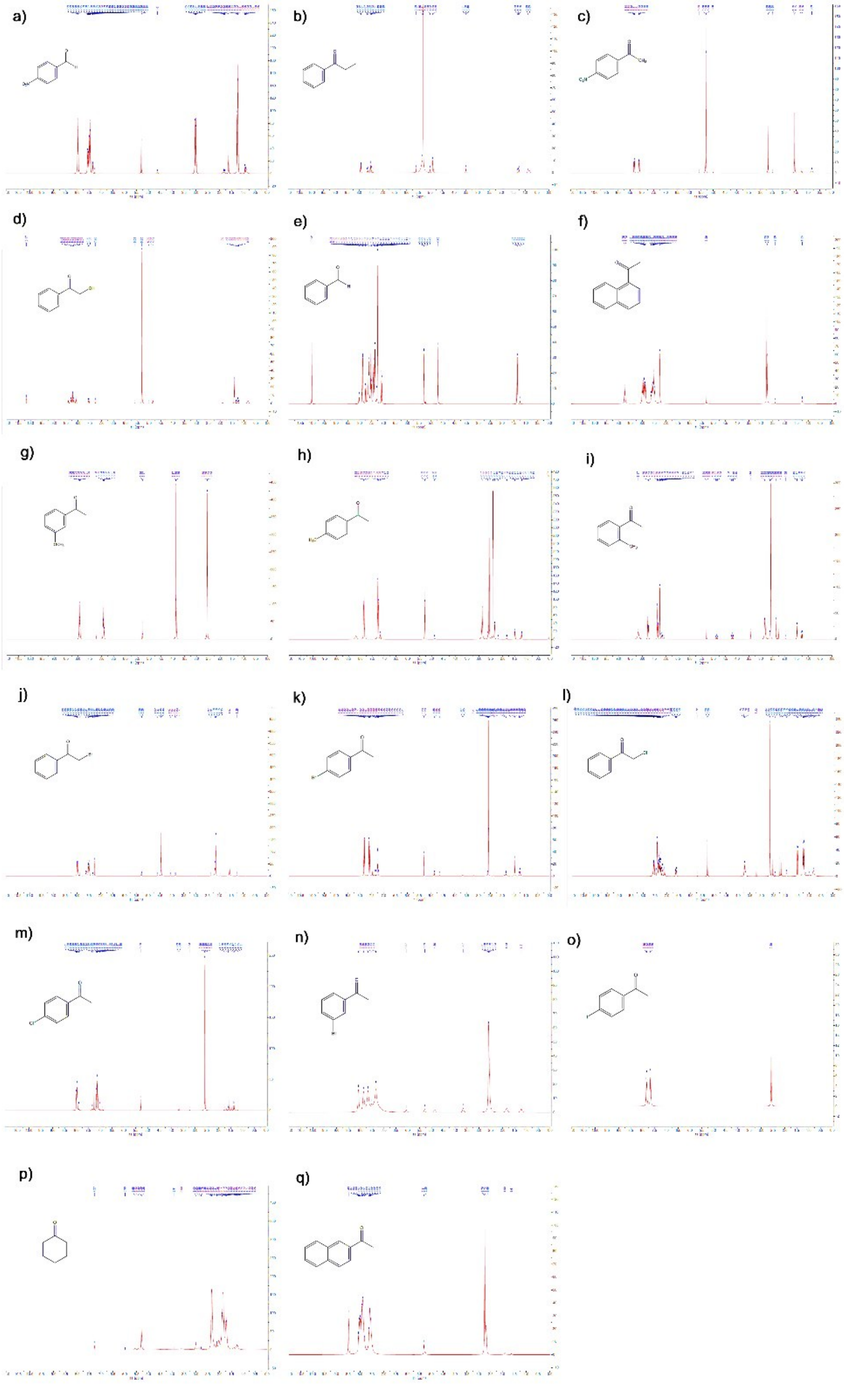

Fig. S14 Various of aryl ketone compounds with HNMR spectrum.

Table S1. Comparison of the conversion and yield data of Ni- or Ru- based nanocatalysts with those found in the literature for transfer hydrogenation.

Catalyst	Cat mol%	Temp. (°C)	Time (h)	Substrate conversion rate (%)	Yield (%)	TON	TOF	Ref.
Ni(10 wt%)@mSiO$_2$	1	100	1	100	99	99	99	This work
Nickel-aluminium alloy	1	100	1	80	62	62	62	
Ni(COD)$_2$	2	130	48	95	95	47.5	0.99	1)
NiCl$_2$(PPh$_3$)$_2$]	1	70	21	93	84	84	4	2)
Ni(OTf)$_2$	5	70	48	85	91	18.2	0.38	3)
NiCl$_2$(DME)	10	115	24	-	95	9.5	0.40	4)
NiBr$_2$(DME)	4	80	12	99	91	22.75	1.90	5)
Ru-TsDPEN-CMS	1	40	3	99	98	98	32.7	6)
[RuCl$_2$(p-cymene)]$_2$	1	rt	1	50	86	86	86	7)
[Ru(benzene)Cl$_2$]$_2$	1	70	21	86	60	60	2.86	8)

References)

1) N. Castellanos-Blanco, A. Arévalo and J. J. Garcia, *Dalton Trans.*, 2016, **45**, 13604-13614

2) Y. Li, S. Yu, W. Shen and J. Gao, *Acc Chem. Res.*, 2015, **48**, 2587-2598

3) P. Yang, L. H. Lim, P. Chuanprasit, H. Hirao and J. S. Zhou, *Angw. Chem. Int. Ed.*, 2016, **55**, 12083-12087

4) B. J. Simmons, M. Hoffman, J. Hwang, M. K. Jackl and N. K. Grag, *Org. Lett.*, 2017, **19**, 1910-1913

5) S. Guo, P. Yang and J. S. Zhou, *Chem. Commun.*, 2015, **51**, 12115-12117

6) R. Liu, T. Cheng, L. Kong, C. Chen, G. Liu and H. Li, *Journal of Catalysis*, 2013, **307**, 55-61

7) Z. Cao, H. Qiao and F. Zeng, *Organometallics*, 2019, **38**, 797-804

8) S. Guillarme, T. X. M. Nguyen and C. Saluzzo, *Tetrahedron: Asymmetry*, 2008, **19**, 1450-1454